Inhibition of ceramide biosynthesis preserves photoreceptor structure and function in a mouse model of retinitis pigmentosa

Enrica Strettoi[a,1], Claudia Gargini[b], Elena Novelli[c], Giusy Sala[d], Ilaria Piano[b], Paolo Gasco[e], and Riccardo Ghidoni[d]

[a]Neuroscience Institute, Consiglio Nazionale delle Ricerche, Pisa 56100, Italy; [b]Department of Psychiatry, Pharmacology, Neurobiology and Biotechnology, University of Pisa, Pisa 56100, Italy; [c]G.B. Bietti Foundation for Ophthalmology, Rome 00198, Italy; [d]Laboratory of Biochemistry and Molecular Biology, San Paolo Medical School, University of Milan, Milan 20142, Italy; and [e]Nanovector srl, Turin 10144, Italy

Edited by Jeremy Nathans, The Johns Hopkins University, Baltimore, MD, and approved September 24, 2010 (received for review June 4, 2010)

Retinitis pigmentosa (RP) is a genetic disease causing progressive apoptotic death of photoreceptors and, ultimately, incurable blindness. Using the retinal degeneration 10 (rd10) mouse model of RP, we investigated the role of ceramide, a proapoptotic sphingolipid, in retinal degeneration. We also tested the possibility that photoreceptor loss can be slowed or blocked by interfering with the ceramide signaling pathway of apoptosis in vivo. Retinal ceramide levels increased in rd10 mice during the period of maximum photoreceptor death. Single intraocular injections of myriocin, a powerful inhibitor of serine palmitoyl-CoA transferase, the rate-limiting enzyme of ceramide biosynthesis, lowered retinal ceramide levels to normal values and rescued photoreceptors from apoptotic death. Noninvasive treatment was achieved using eye drops consisting of a suspension of solid lipid nanoparticles loaded with myriocin. Short-term noninvasive treatment lowered retinal ceramide in a manner similar to intraocular injections, indicating that nanoparticles functioned as a vector permitting transcorneal drug administration. Prolonged treatment (10–20 d) with solid lipid nanoparticles increased photoreceptor survival, preserved photoreceptor morphology, and extended the ability of the retina to respond to light as assessed by electroretinography. In conclusion, pharmacological targeting of ceramide biosynthesis slowed the progression of RP in a mouse model, and therefore may represent a therapeutic approach to treating this disease in humans. Transcorneal administration of drugs carried in solid lipid nanoparticles, as experimented in this study, may facilitate continuous, noninvasive treatment of patients with RP and other retinal pathologies.

sphingolipid | apoptosis | electroretinography | morphology

Retinitis pigmentosa (RP), one of the leading causes of blindness worldwide, comprises numerous retinal dystrophies of genetic origin frequently caused by mutations in genes essential to rod photoreceptor function and metabolism, resulting in rod cell death and subsequent night blindness (1). Progressively, cone photoreceptors also die, until all useful sight is lost. Although there is presently no cure for RP, substantial progress has been made to elucidate the genetics and cell biology of these disorders. In particular, rod photoreceptor death in RP is largely thought to occur by apoptosis (2–5), although nonapoptotic mechanisms have also been proposed (5).

Among known proapoptotic cellular messengers, the sphingolipid ceramide is a well-characterized death effector in various experimental models and pathological conditions (6–9). Endogenous cellular levels of ceramide increase after stimulation with different proapoptotic factors that cause acute and chronic disease (10, 11). This increase in ceramide can originate from an activation of de novo biosynthesis, a rise in ceramide hydrolysis from sphingomyelin by the action of neutral or acid sphingomyelinases, or a decrease in ceramide metabolism due to glycosylation, phosphorylation, or deacetylation (12). An important role for ceramide-mediated apoptosis in neurodegenerative and neuroinflammatory diseases has now been established (10).

Several lines of evidence suggest that ceramide also mediates apoptosis in retinal photoreceptors (13). First, in *Drosophila* models of RP, genetic manipulation of sphingolipid metabolism has protective effects on retinal morphology and function; protection was achieved both by expressing neutral ceramidase in *Drosophila* eye, to reduce cellular levels of ceramide, and by knocking out one copy of a gene encoding a subunit of serine palmitoyl-CoA transferase (SPT), the enzyme that controls the rate-limiting step of ceramide biosynthesis (14). In humans, a direct genetic link between retinal degeneration and sphingolipid-mediated apoptosis has been established with the discovery that a loss-of-function mutation in CERKL, a gene expressing ceramide kinase-like protein, caused autosomal recessive RP (15, 16), although debate exists on the pathway leading to cell death in individuals with this mutation (17). In rat retinal neuronal primary cultures, oxidative stress increased ceramide levels and caused apoptosis, whereas these effects were blocked by addition of docosahexaenoic acid to stimulate antiapoptotic responses (18). Similarly, in the murine 661W photoreceptor cell line, oxidative stress stimulated acid sphingomyelinase and increased ceramide levels, thereby activating the mitochondrial apoptotic pathway and the caspase cascade (19). Finally, in a rabbit model of retinal apoptosis, ceramide increased after experimental retinal detachment (20). Altogether, these studies document that the accumulation of ceramide is associated with retinal degeneration and suggest that pharmacological interventions altering sphingolipid metabolism may have therapeutic potential.

Effective RP therapies might be implemented on biological models that accurately represent retinal degeneration in humans. Recently, the retinal degeneration 10 (rd10) mouse, with a missense mutation in the β-subunit of the rod-specific phosphodiesterase gene (21), has been shown, through morphological and functional retinal analyses, to be a faithful model of typical human RP (22, 23). In this mutant, photoreceptors begin to die from apoptosis during the third week of life, after the postnatal period of retinal maturation, and photoreceptor death peaks around postnatal day 24 (P24) (22, 23). As in typical human RP, rods die first, whereas cones are lost subsequently. Morphologically, the loss of photoreceptors is accompanied by a progressive thinning of the outer retina and consequent reduction in the number of photoreceptor rows from 12 to 14 on P10 to only 2–3 rows on P30. Functionally, rod-mediated retinal responses to

Author contributions: E.S., C.G., P.G., and R.G. designed research; E.S., C.G., E.N., G.S., I.P., and R.G. performed research; P.G. contributed new reagents/analytic tools; E.S., C.G., E.N., G.S., I.P., and R.G. analyzed data; and E.S., C.G., and R.G. wrote the paper.

Conflict of interest statement: E.S., C.G., P.G., and R.G. filed a patent for the employment of inhibitors of serine palmitoyltransferase in retinitis pigmentosa (Patent MI2009A000284). P.G. is employed by Nanovector srl, Turin, Italy.

This article is a PNAS Direct Submission.

[1]To whom correspondence should be addressed. E-mail: enrica.strettoi@in.cnr.it.

This article contains supporting information online at www.pnas.org/lookup/suppl/doi:10.1073/pnas.1007644107/-/DCSupplemental.

light are measurable by electroretinography (ERG) from P14 (the day of eye opening) until P28, although the responses are slow and weak compared with those of wild-type mice (23).

The availability of the rd10 mouse model of RP permitted us to investigate whether pharmacological treatment with myriocin, a selective inhibitor of SPT, could reduce ceramide and thereby exert a protective effect against retinal degeneration. Myriocin, a fungal metabolite discovered for its immunosuppressant properties, is an atypical amino acid with a long hydrophobic tail, structurally similar to sphingosine (24). To our knowledge, myriocin has never been tested for protective effects on retinal degeneration. Here we show that retinas of rd10 mice pups have unusually high levels of ceramide which can be reduced by topical administration of myriocin, concomitantly obtaining both protection of photoreceptors from apoptotic death and maintenance of ERG functional response. Furthermore, we show that noninvasive drug delivery can be achieved using eye drops containing a suspension of myriocin-loaded solid lipid nanoparticles.

Results

To determine whether, in the rd10 mouse model of RP, there are altered levels of retinal ceramide, retinas were obtained between P12 and P30 from rd10 mice pups and from wild-type animals of the same genetic background. Total retinal ceramide, normalized to the amount of inorganic phosphate (Pi) from total phospholipid, was similar in the two groups until P16, after which ceramide content started to increase in rd10 animals but continued to slowly decrease in wild-type mice (Fig. 1*A*). Significant differences between wild-type and rd10 mice were observed at P21 ($P = 0.045$, t test) and P30 ($P = 0.001$), that is, during the period of maximum retinal degeneration in rd10 mice. To test whether these pathologically high levels could be reduced pharmacologically, we administered myriocin by intraocular injection on P19 followed by ceramide quantification on P21. In 14 of 16 mice, myriocin injection into the right vitreous body reduced retinal ceramide levels below that of the left eye, injected with vehicle alone (Fig. 1*B*). Overall, myriocin induced a 25.4% reduction in mean ceramide content, from 4.09 pmol/nmol Pi (SD = 1.16) to 3.05 pmol/nmol Pi (SD = 0.97) ($P = 0.011$, paired t test). This treatment was therefore effective in bringing ceramide to levels considered normal for P21. Similar treatment of wild-type mice also reduced ceramide content, by 17.5%, from a mean of 2.00 pmol/nmol Pi (SD = 0.34) to 1.65 pmol/nmol Pi (SD = 0.12) ($P = 0.032$, paired t test).

A possible protective effect of intraocular myriocin injection on photoreceptor survival was investigated by assessing the relative abundance of apoptotic photoreceptors in retinas from myriocin- and DMSO-treated eyes. Isolated retinas were stained with a fluorescent nuclear dye to identify pycnotic (condensed) nuclei and visualized with confocal microscopy. Retinas from myriocin-treated right eyes had fewer intensely stained nuclei than vehicle-treated left eyes (Fig. 2 *A* and *B*). Quantitative analysis revealed that 2 d after a single myriocin injection, the number of pycnotic photoreceptor nuclei was reduced by 52.6% ($P = 0.007$, t test) (Fig. 2*C*). To determine whether these protective cellular effects were associated with a maintenance of retinal function, we measured electrical responses to light by ERG 2 d after a single injection of drug or vehicle. ERG traces from myriocin-treated eyes overlapped with those from DMSO-treated eyes (Fig. S1). Thus, despite a preservation of cellular viability, a single injection of myriocin did not have measurable functional benefits.

Recognizing that continual pharmacological treatment may be necessary to achieve positive effects on retinal function, we topically administered 0.5 nmol myriocin (1 μL of 3.77 mM solution in DMSO) to the cornea of rd10 mice once daily for 4 d. Microscopic analysis for pycnotic nuclei and ceramide quantification revealed no significant difference between myriocin- and DMSO-treated retinas, suggesting that the drug did not cross the cornea. Therefore, we investigated the possibility of using solid lipid nanoparticles (SLNs) as vehicle to carry the drug across ocular tissues; SLNs are pure lipid particles with a diameter of 40–200 nm. First, we assessed the ability of fluorescently labeled SLNs to reach the interior of the mouse eye. SLNs labeled with the hydrophobic dye *N*-(7-nitro-2-1,3-benzoxadiazol-4-yl)-1,2-dipalmitoyl-*sn*-glycero-3-phosphoethanolamine (NBD-DPPE) were topically applied to the ocular surface of wild-type mice once daily for 3 d. Confocal microscopy of vertical retinal slices revealed the presence of bright aggregates inside the retina (absent from eyes treated with unlabeled SLNs), mostly in the outer nuclear layer (ONL) and also between the photoreceptors and the retinal pigment epithelium (Fig. 3*A*). Spectral analysis confirmed that the observed aggregates contained the NBD-DPPE fluorophore (Fig. 3*B*). Similar observations were obtained for SLNs labeled with coumarin and Nile red. These results demonstrated the feasibility of using SLNs to deliver small, lipophilic molecules across the cornea to the photoreceptors and to the retinal pigment epithelium.

SLNs were subsequently prepared with myriocin. The concentration of the drug in different preparations, considered suitable for use in rd10 mice, ranged from 0.4 to 1.0 mM (mean, 0.6 mM). Myriocin-SLNs were administered topically to both corneas of rd10 mice, three times per day for 3 d starting on P19; additional rd10 mice were treated with control SLNs. In retinas collected on P21, mean values of ceramide were 2.49 pmol/nmol Pi (SD = 0.25) in myriocin-treated animals but 4.19 pmol/nmol Pi (SD = 0.92) in control animals ($P < 0.001$, t test). These results document that myriocin can be effectively administered across the cornea when incorporated into SLNs. However, despite the fact that this treatment reduced retinal ceramide by 40.6% (even more than with a single intraocular injection), still no significant effect was observed on retinal functional responses. Therefore, long-term treatment with myriocin-SLNs was investigated.

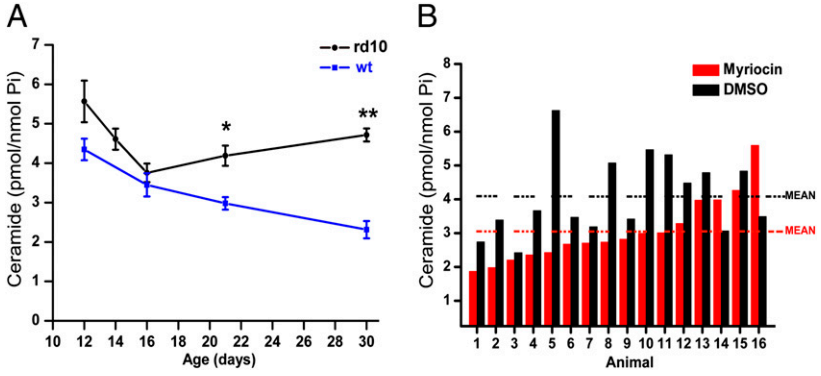

Fig. 1. Ceramide content in mouse retina and effect of myriocin. (*A*) Time course of endogenous ceramide content in retinas of mice pups during the first month of life: in rd10 mice, ceramide levels begin to increase during the third week of life, in concomitance with retinal degeneration. Values are mean and SE of three to five retinas per data point. *$P = 0.050$; **$P = 0.001$, t test. (*B*) Effect of intraocular myriocin injection on retinal ceramide content in rd10 mice. Right eyes were injected on P19 with a single dose of myriocin; left eyes were treated with vehicle. Ceramide content was assessed on P21. Animals are shown in order of increasing ceramide content in myriocin-treated retinas. In 14 of 16 animals, myriocin lowered ceramide content; $P = 0.030$, paired t test.

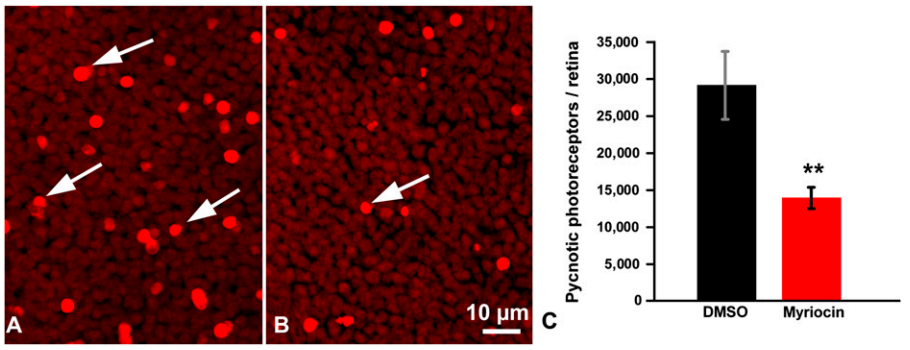

Fig. 2. Intraocular myriocin injection slows photoreceptor loss. (*A* and *B*) Fluorescence microscopy of retina whole mounts, fixed and stained with ethidium homodimer, from mice treated with vehicle (*A*) or myriocin (*B*) on P19. Myriocin injection was associated with a reduction in the number of pycnotic photoreceptor nuclei on P21. (*C*) Quantification of pycnotic nuclei per retina. Values are mean (SE) of 16 mice. $^{**}P = 0.007$, *t* test.

Starting on P14, rd10 and wild-type (control) mice were treated once daily with myriocin-SLNs or control SLNs. From P21 to P35, different animals underwent ERG testing of retinal function followed by retinal microscopic analysis. Myriocin treatment in wild-type animals had no effect on ERG, which showed the typically large amplitudes of a and b waves (Fig. S2). In both control and myriocin-treated rd10 mice, mean amplitudes of ERG b waves decreased progressively over time in concomitance with retinal degeneration; similar results were observed for absolute values of mean ERG a waves (Fig. 4). However, absolute values of the mean amplitudes were larger in myriocin-treated than control animals at all time points except P35, when b-wave amplitudes were essentially identical. Significant differences between the two groups were observed for a-wave amplitudes at P30 and P35. These results indicate that continual topical application of myriocin-SLNs can counteract, to a certain extent, the loss of function due to photoreceptor death in rd10 mice.

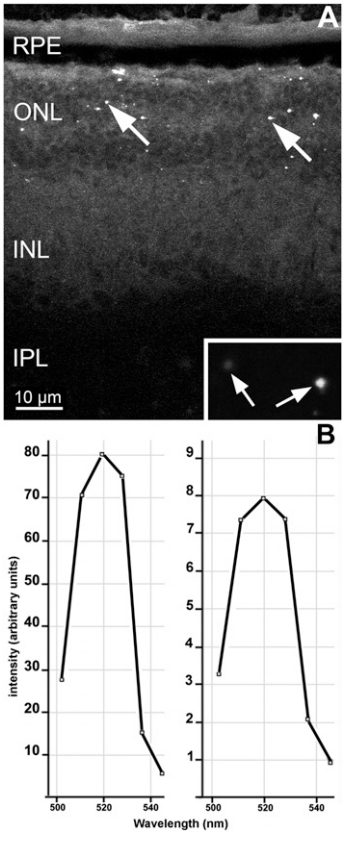

Fig. 3. Topically administered SLNs reach retinal photoreceptors. (*A*) Fluorescence microscopy of a vertical section of wild-type mouse retina, 3 d after repeated topical application of SLNs labeled with the hydrophobic fluorescent dye NBD-DPPE: bright puncta (arrows) are seen in the outer nuclear layer (ONL) and between photoreceptors and the retinal pigment epithelium (RPE). (*Inset*) High-magnification of fluorescent puncta of different brightness. INL, inner nuclear layer; IPL, inner plexiform layer. (*B*) Fluorescence emission spectra from a smear of NBD-DPPE-labeled SLNs (*Left*) and from puncta in retinal sections of treated mice (*Right*). The two spectra have the same shape and peak emission at 520 nm, similar to that of NBD-DPPE (39).

The maximum effects of myriocin treatment on retinal responses to light of increasing intensity are illustrated in Fig. 5, which shows ERG traces from two rd10 mice pups treated for 10 d (P14–P24) with either myriocin-SLNs or control SLNs. In the myriocin-treated animal, there is higher preservation of both a and b waves of the ERG.

To assess the morphological effects of treatment with myriocin-SLNs on photoreceptors, we counted the number of photoreceptor rows in the outer nuclear layer, considered a more sensitive measure of photoreceptor survival over long periods of treatment than the number of pycnotic nuclei. Microscopic analysis of vertical retinal sections revealed a protective effect of myriocin on the number of photoreceptor rows, seen as a thicker cross-section of the outer nuclear layer (Fig. 6*A*). This effect was significant at both P24 and P30 (Fig. 6*B*). The morphology of surviving photoreceptors was preserved as well, as documented by the presence of rhodopsin and cone opsin immunoreactivity in well-organized outer segments of rods and cones, by retention of synaptic terminals of these cells, and by the presence of well-organized dendrites in rod bipolar cells (Fig. S3).

Finally, in a preliminary assessment of safety of long-term treatment, eyes from anesthetized rd10 and wild-type mice treated for 14 d with myriocin-SLNs were examined under a dissection microscope before enucleation for signs of conjunctiva irritation/edema, which were absent. Cataract and corneal opacities could be excluded by the fact that we successfully recorded ERGs. Nuclear staining of retinal sections with ethidium revealed normal retinal histology. Immunohistochemical analyses did not reveal macrophage infiltration (which would have indicated inflammation) nor microglial activation (Fig. S4).

An extension of beneficial effects of myriocin-SLN treatment to retinal cones is anticipated by the morphological preservation of these cells in myriocin-SLN-treated retinas, as well as the recording of a larger cone-driven ERG in rd10 mice treated with myriocin-SLNs for 26 d, compared with control animals (Figs. S3*B* and S5).

Discussion

This study found that, in the rd10 mouse model of RP, the level of retinal ceramide begins to increase from the third week of life, during the period of maximum photoreceptor loss, whereas in wild-type mice ceramide levels progressively decrease. Single intraocular injections of myriocin, a selective inhibitor of SPT, the rate-limiting enzyme of ceramide biosynthesis, decreased

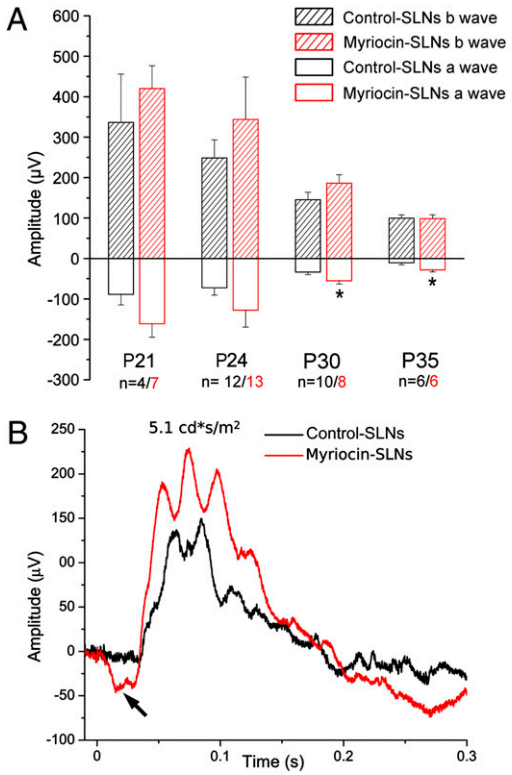

Fig. 4. Effects of long-term administration of myriocin-SLNs on retinal physiology. (*A*) Amplitudes of ERG a and b waves from eyes of rd10 mice treated with control SLNs or myriocin-SLNs from P14 and exposed to a light flash of 5.1 cd·s/m^2. Values are mean and SE. Mice treated with myriocin-SLNs (red bars) have larger mean a-wave amplitudes at P30 and P35 (*P = 0.050, Wilcoxon–Mann–Whitney test). (*B*) Representative ERG responses to light from two rd10 mice treated for 10 d (from P14 to P24) with myriocin-SLNs (red trace) or control SLNs (black trace). Note the preservation of the a wave following myriocin treatment (arrow).

retinal ceramide and reduced the number of apoptotic photoreceptors in the short term. A functional benefit of myriocin was observed after prolonged daily treatment, achieved by the noninvasive, transcorneal administration of the drug contained in solid lipid nanoparticles. In rd10 mice treated with myriocin-SLNs for 10–20 d, the pathological decrease in photoreceptor number was slowed, photoreceptor morphology was preserved, and the degeneration of retinas was delayed.

The finding that ceramide levels increase in the rd10 mouse in temporal association with the process of photoreceptor demise (22, 23) provides biochemical evidence that this sphingolipid is involved in the neurodegenerative pathology of RP. This result is therefore in accordance with the knowledge derived from genetic studies that human autosomal recessive RP can be caused by loss-of-function mutations in *CERKL*, an enzyme that lowers ceramide content by phosphorylation (15). The results are also in agreement with the increased ceramide levels found in tissues from individuals with other pathologies leading to apoptosis, such as brain tissue from Alzheimer's disease patients (25), and thus provide additional evidence that elevated ceramide is a pathogenetic factor of various diseases. Moreover, the fact that in vivo reduction of retinal ceramide levels slowed disease progression extends to mammals earlier results obtained in *Drosophila* models of RP (14). Therefore, these experiments provide a proof of principle that ceramide regulation represents a relevant therapeutic target in RP as in other pathologies (6, 12, 26–30). Compared with a previous study in *Drosophila* models of RP (14), in which retinal ceramide levels were lowered by genetic manipulation, in this study ceramide levels were lowered pharmacologically. Because noninvasive pharmacological intervention is more easily achieved in humans than gene therapy, the strategy proposed here might become applicable to humans in the long run.

A functional benefit of myriocin was observed only after prolonged treatment but not after a single intraocular administration, despite the fact that both administration methods reduced ceramide levels. The lack of measurable functional effects of single myriocin administrations might be ascribed to the small proportion of photoreceptors rescued from apoptotic death in the short period of study (2 d). Possibly the corresponding effect on the ERG fell below the sensitivity of this functional test.

This study has a few limitations, the most evident being that chronic administration of myriocin rescued a fraction of photoreceptors for a limited time, mostly delaying the inevitable death process in these cells. However, it has to be considered that prolonging the natural evolution of a disease like RP, which characteristically exhibits a slow progression, can nonetheless be beneficial for patients. Another limitation is that we studied a single genetic paradigm of RP, whereas it is known that this disease is genetically heterogeneous. Different mutations leading to photoreceptor demise could activate different pathways of apoptosis (31), within which the sphingolipidic cascade could play more or less relevant roles, which need to be studied.

Overall, the results described here are particularly encouraging, considering that the partial loss-of-function rd10 mutation mimics typical RP forms with moderately aggressive phenotype and good retention of retinal architecture (23). These are features that portray human RP patients as likely candidates for gene therapy, in which the defective gene is replaced by a functioning one by means of genetically engineered viral vectors (32). A protective pharmacological approach, based on the noninvasive administration of SPT inhibitors, could prolong the lifespan of photoreceptors in recessive forms of RP, pending gene therapy at a later stage. SPT inhibitors similar to myriocin could therefore contribute to enlarge the panel of bioactive substances already used as neuroprotectants to delay photoreceptor death in this disease (33, 34). In addition, considering that an increment in the rate of rod survival is known to promote a proportionally longer viability of cones, essential for daylight vision, it is possible that the beneficial effects of delaying the sphingolipid-mediated rod demise would propagate to cones as well. Finally, the particular pharmacological strategy used here, based on the employment of lipophilic, tissue-permeant drops, represents a suitable method to deliver molecules to the inner eye noninvasively. Various carriers (i.e., bio- and nonbiodegradable implants, microspheres, nanoparticles, liposomes, and gels) have been tested experimentally to deliver drugs to the inner eye (35). The particular advantages of the SLNs used here are their lack of undesirable effects and their suitability for carrying nonpolar, lipophilic compounds. These features can be exploited for drug delivery in retinal disorders other than RP.

In conclusion, this study demonstrates that pharmacological targeting of ceramide biosynthesis has the potential to slow the progression of RP in a mammalian model and therefore may represent a therapeutic approach to treating this disease in humans. Transcorneal administration of drugs carried in solid lipid nanoparticles, as experimented in this study, may also be developed for human patients with other ocular disorders requiring therapy with lipophilic molecules.

Methods

Animals. rd10 mice (Jackson Laboratories strain B6.CXB1-*Pde6b*^{rd10}/J) (36) and wild-type mice (Jackson Laboratories strain C57BL/6J) were kept in a local facility with water and food ad libitum in a 12-h light/dark cycle with illumination level below 60 lux. Mice were handled according to Italian laws and following the Association for Research in Vision and Ophthalmology

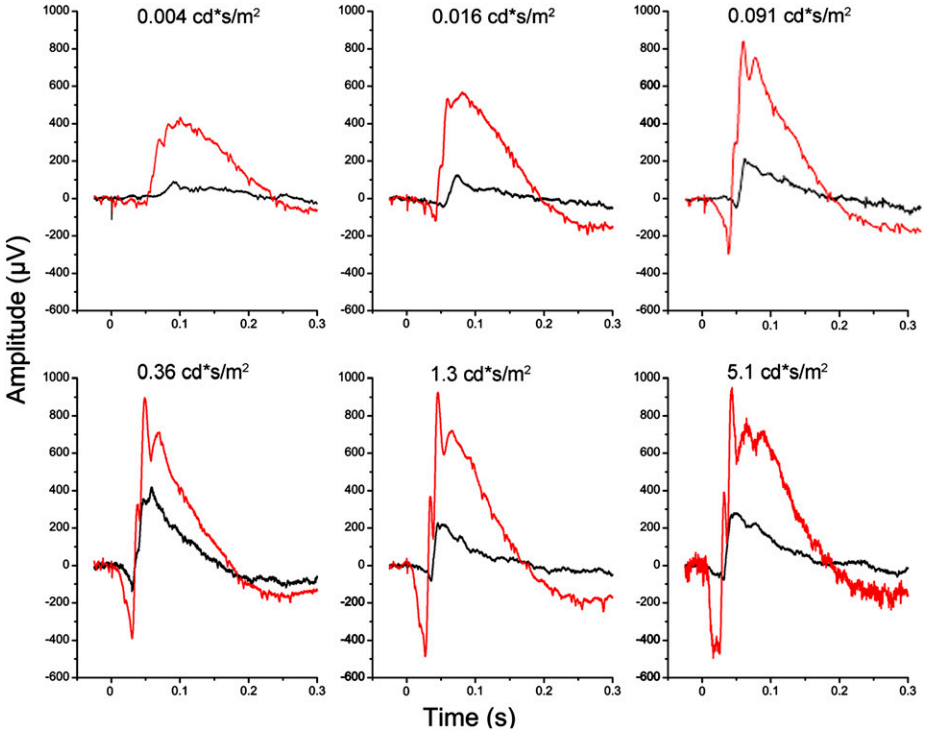

Fig. 5. Effects of myriocin-SLNs on ERG. The best examples of ERG responses to flashes of light of increasing intensity from two rd10 mice age P24. Traces in the panel corresponding to the lowest light intensity are purely rod-driven, whereas the others represent mixed rod–cone responses. Red traces, responses from a mouse treated with myriocin-SLNs; black traces, responses from a mouse treated with control SLNs. In this instance, the SLNs contained the highest myriocin concentration (1 mM) of this study.

(ARVO) statement for the use of animals in research. Protocols were approved by the Italian Ministry of Veterinary Health.

Quantification of Retinal Ceramide. Mice were anesthetized with an i.p. injection of avertin (0.5 g/mL 2,2,2-tribromoethanol in ter-amylic alcohol; 20 μL/g body weight). Eyes were quickly removed and retinas were detached, placed in oxygenated artificial cerebral-spinal fluid medium, and frozen on dry ice. Retinal lipid was extracted using the Bligh–Dyer method, and total phospholipid was quantified using the Ames method of Pi determination. Ceramide was determined by diglyceride kinase assay (*SI Methods*).

Intraocular Injections. Mice were anesthetized as above. Using a dissecting microscope, 500 nL of a 1.88 mM solution of myriocin in DMSO was injected into the right vitreous body using a 10-μL glass Hamilton syringe driven by an oil microinjector. Considering that the injected volume is diluted seven- to eightfold within the vitreous body (37), this dosage provides an intraocular concentration of ≈0.23 mM myriocin, one order of magnitude higher than that used to inhibit SPT enzymatic activity in single-layer cell-culture studies (38). An identical volume of DMSO vehicle was injected into the left eyes of the same animals.

Fluorescence Microscopy of Retinas for Pycnotic Photoreceptors. Mice were anesthetized as described earlier, and eyes were enucleated and fixed with 4% paraformaldehyde in 0.1 M sodium phosphate (pH 7.2). Retinas were detached and stained with 2 μM ethidium homodimer 2 (Invitrogen), a fluorescent DNA-intercalating molecule to which fixed tissue is permeable. Whole-mounted retinas were examined under a Leica TCS-SP confocal microscope for the presence of pycnotic (apoptotic) photoreceptor nuclei, brighter than others in the same layer because of the high density of their

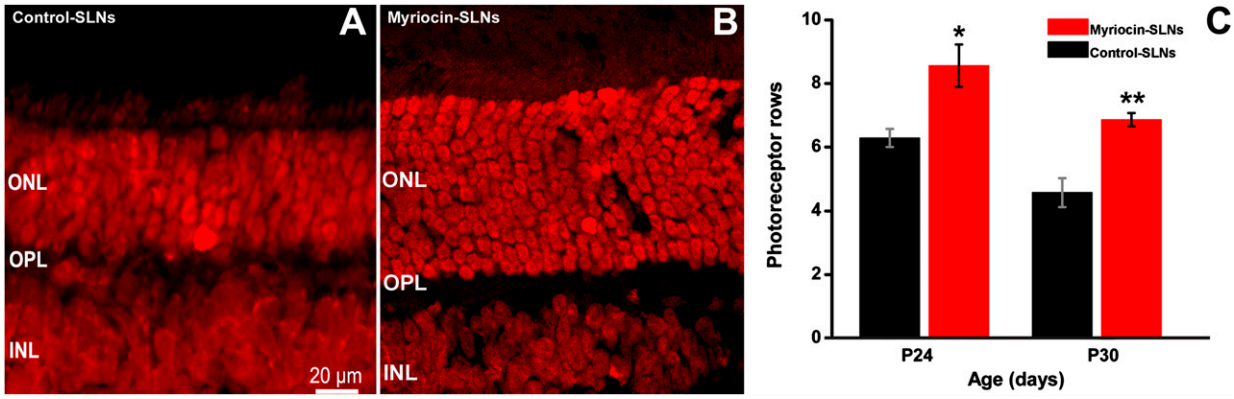

Fig. 6. Effects of myriocin-SLNs on retinal morphology. (*A* and *B*) Vertical retinal sections from rd10 mice treated with control SLNs (*A*) and myriocin-SLNs (*B*) for 10 d (from P14 to P24). The outer nuclear layer (ONL) of the myriocin-treated retina is thicker because it contains more photoreceptor rows than the control retina. These micrographs are from the same animals whose ERG data are shown in Fig. 4*B*. INL, inner nuclear layer; OPL, outer plexiform layer. (*C*) Quantification of photoreceptor rows at P24 and P30 in rd10 mice treated with control SLNs or myriocin-SLNs. Data are mean and SE. $*P = 0.002$, $**P = 0.003$, *t* test.

condensed DNA. The ONL, containing the nuclei of photoreceptors, was sampled along the whole *z* axis. Photoreceptor pycnotic nuclei were counted on projection images of the ONL in fields of 150.6 × 150.6 μm^2 (32 fields/retina), spaced at 500-μm intervals along the dorsal-ventral and nasal-temporal retinal meridians. The total number of pycnotic photoreceptors for each retina was calculated by multiplying the average density of pycnotic cells in field images by the corresponding retinal area, measured by low-power light microscopy with an image analyzer (Metamorph 5.0, Universal Imaging Corporation).

Electroretinography. Retinal viability and function were assessed by recording flash electroretinograms as previously described (23); details are given in *SI Methods*. When using mice treated with SLNs, ERG traces were recorded simultaneously from both eyes, identically treated. The possible diffusion of SLNs from one eye to the other made it necessary to use different mice for control and experimental treatments.

Solid Lipid Nanoparticles. Noninvasive, transcorneal treatment of mouse retina was achieved with the use of SLNs, patented by Nanovector srl (*SI Methods*) (40). The concentration of myriocin in SLN preparations was determined by extraction with chloroform:methanol:37% HCl (100:200:1 by volume) followed by TLC on silica gel plates in l-butanol:acetic acid:water (3:1:1 by volume). Known amounts of myriocin were loaded on the same TLC plate to generate a standard curve. Separated lipids were visualized by staining with an aqueous solution of 10% $CuSO_4$, 8% H_3PO_2 on a hot plate (180 °C) for 3–6 min. Myriocin spots were quantified by densitometry (Gel Doc 2000 and Quantity One software; Bio-Rad).

Topical Administration of SLNs. To determine whether lipophilic molecules contained in SLNs penetrate the inner eye, wild-type mice were treated three times per day with 1 μL SLNs labeled with coumarin, Nile red, or NBD-DPPE; unlabeled SLNs served as control. After 3 d of treatment, vertical retina sections were examined by fluorescence confocal microscopy for the presence and localization of the fluorophore within the retina. To determine whether the observed fluorescence corresponded to the fluorophore administered topically, the emission spectrum from retinal sections was compared with that of a smear of the SLNs on a microscope slide by fluorescent spectral analysis using the confocal microscope's 488-nm laser source. For pharmacological treatment, rd10 mice (66 animals from 10 litters) and wild-type mice (n = 12) were administered once daily with either myriocin-SLNs or control SLNs in both eyes. Each treatment consisted of a double dosage, within a 15-min interval, of 750–1,000 nL/eye (larger volumes were used in older animals). Treatment started on P14 (eye opening) and continued until analysis between P21 and P35.

Fluorescence Microscopy on Retinal Vertical Sections. Retinas from rd10 and wild-type mice that had been treated with SLNs were harvested for morphological analysis. Photoreceptor survival was assessed by counting nuclei in the ONL. Photoreceptor morphology was assessed by immunohistochemistry (*SI Methods*).

Statistical Analysis. Data were compared by two-tailed unpaired or paired *t* tests or with the Wilcoxon–Mann–Whitney test when the distribution of data was not normal, as assessed by analysis with SigmaStat v. 3.1 (Systat). Statistical analysis was performed with Origin v. 7.0 (OriginLab) and SigmaStat v. 3.1 software packages for Windows XP. A P value <0.05 was considered significant.

ACKNOWLEDGMENTS. The authors are indebted to P. Signorelli for discussion, M. Ferraroni for guidance with statistical analysis, A. Asta for technical support, and L. Cervetto for invaluable suggestions and support throughout the study. V. Matarese provided editorial advice and scientific editing. This work was supported by the British Retinitis Pigmentosa Society, 2007 National Interest Research Project (PRIN) of the Italian Ministry of Education (MIUR), Banco del Monte di Lombardia, the Italian National Research Council (CNR), the Universities of Milan and Pisa, and National Institutes of Health Grant R01 EY12654 (to E.S.).

1. Hartong DT, Berson EL, Dryja TP (2006) Retinitis pigmentosa. *Lancet* 368:1795–1809.
2. Corrochano S, et al. (2008) Attenuation of vision loss and delay in apoptosis of photoreceptors induced by proinsulin in a mouse model of retinitis pigmentosa. *Invest Ophthalmol Vis Sci* 49:4188–4194.
3. Cottet S, Schorderet DF (2009) Mechanisms of apoptosis in retinitis pigmentosa. *Curr Mol Med* 9:375–383.
4. Portera-Cailliau C, Sung CH, Nathans J, Adler R (1994) Apoptotic photoreceptor cell death in mouse models of retinitis pigmentosa. *Proc Natl Acad Sci USA* 91:974–978.
5. Sancho-Pelluz J, et al. (2008) Photoreceptor cell death mechanisms in inherited retinal degeneration. *Mol Neurobiol* 38:253–269.
6. Billich A, Baumruker T (2008) Sphingolipid metabolizing enzymes as novel therapeutic targets. *Subcell Biochem* 49:487–522.
7. Deng X, et al. (2008) Ceramide biogenesis is required for radiation-induced apoptosis in the germ line of *C. elegans*. *Science* 322:110–115.
8. Hannun YA, Obeid LM (2008) Principles of bioactive lipid signalling: Lessons from sphingolipids. *Nat Rev Mol Cell Biol* 9:139–150.
9. Morales A, Lee H, Goñi FM, Kolesnick R, Fernandez-Checa JC (2007) Sphingolipids and cell death. *Apoptosis* 12:923–939.
10. Jana A, Hogan EL, Pahan K (2009) Ceramide and neurodegeneration: Susceptibility of neurons and oligodendrocytes to cell damage and death. *J Neurol Sci* 278:5–15.
11. Toman RE, Spiegel S, Faden AI (2000) Role of ceramide in neuronal cell death and differentiation. *J Neurotrauma* 17:891–898.
12. Kitatani K, Idkowiak-Baldys J, Hannun YA (2008) The sphingolipid salvage pathway in ceramide metabolism and signaling. *Cell Signal* 20:1010–1018.
13. Rotstein NP, Miranda GE, Abrahan CE, German OL (2010) Regulating survival and development in the retina: Key roles for simple sphingolipids. *J Lipid Res* 51: 1247–1262.
14. Acharya U, et al. (2003) Modulating sphingolipid biosynthetic pathway rescues photoreceptor degeneration. *Science* 299:1740–1743.
15. Avila-Fernandez A, et al. (2008) CERKL mutations and associated phenotypes in seven Spanish families with autosomal recessive retinitis pigmentosa. *Invest Ophthalmol Vis Sci* 49:2709–2713.
16. Tuson M, Marfany G, Gonzàlez-Duarte R (2004) Mutation of CERKL, a novel human ceramide kinase gene, causes autosomal recessive retinitis pigmentosa (RP26). *Am J Hum Genet* 74:128–138.
17. Graf C, Niwa S, Müller M, Kinzel B, Bornancin F (2008) Wild-type levels of ceramide and ceramide-1-phosphate in the retina of ceramide kinase-like-deficient mice. *Biochem Biophys Res Commun* 373:159–163.
18. German OL, Miranda GE, Abrahan CE, Rotstein NP (2006) Ceramide is a mediator of apoptosis in retina photoreceptors. *Invest Ophthalmol Vis Sci* 47:1658–1668.
19. Sanvicens N, Cotter TG (2006) Ceramide is the key mediator of oxidative stress-induced apoptosis in retinal photoreceptor cells. *J Neurochem* 98:1432–1444.
20. Ranty ML, et al. (2009) Ceramide production associated with retinal apoptosis after retinal detachment. *Graefes Arch Clin Exp Ophthalmol* 247:215–224.
21. Chang B, et al. (2007) Two mouse retinal degenerations caused by missense mutations in the β-subunit of rod cGMP phosphodiesterase gene. *Vision Res* 47:624–633.
22. Barhoum R, et al. (2008) Functional and structural modifications during retinal degeneration in the rd10 mouse. *Neuroscience* 155:698–713.
23. Gargini C, Terzibasi E, Mazzoni F, Strettoi E (2007) Retinal organization in the retinal degeneration 10 (rd10) mutant mouse: A morphological and ERG study. *J Comp Neurol* 500:222–238.
24. Miyake Y, Kozutsumi Y, Nakamura S, Fujita T, Kawasaki T (1995) Serine palmitoyltransferase is the primary target of a sphingosine-like immunosuppressant, ISP-1/myriocin. *Biochem Biophys Res Commun* 211:396–403.
25. He B, Lu N, Zhou Z (2009) Cellular and nuclear degradation during apoptosis. *Curr Opin Cell Biol* 21:900–912.
26. Claus RA, Dorer MJ, Bunck AC, Deigner HP (2009) Inhibition of sphingomyelin hydrolysis: Targeting the lipid mediator ceramide as a key regulator of cellular fate. *Curr Med Chem* 16:1978–2000.
27. Liu X, et al. (2008) Acid ceramidase inhibition: A novel target for cancer therapy. *Front Biosci* 13:2293–2298.
28. McEachern KA, et al. (2007) A specific and potent inhibitor of glucosylceramide synthase for substrate inhibition therapy of Gaucher disease. *Mol Genet Metab* 91:259–267.
29. Ozbayraktar FB, Ulgen KO (2009) Molecular facets of sphingolipids: Mediators of diseases. *Biotechnol J* 4:1028–1041.
30. Schenck M, Carpinteiro A, Grassmé H, Lang F, Gulbins E (2007) Ceramide: Physiological and pathophysiological aspects. *Arch Biochem Biophys* 462:171–175.
31. Marigo V (2007) Programmed cell death in retinal degeneration: Targeting apoptosis in photoreceptors as potential therapy for retinal degeneration. *Cell Cycle* 6:652–655.
32. Cai X, Conley SM, Naash MI (2009) RPE65: Role in the visual cycle, human retinal disease, and gene therapy. *Ophthalmic Genet* 30:57–62.
33. Komeima K, Rogers BS, Campochiaro PA (2007) Antioxidants slow photoreceptor cell death in mouse models of retinitis pigmentosa. *J Cell Physiol* 213:809–815.
34. Sieving PA, et al. (2006) Ciliary neurotrophic factor (CNTF) for human retinal degeneration: Phase I trial of CNTF delivered by encapsulated cell intraocular implants. *Proc Natl Acad Sci USA* 103:3896–3901.
35. Janoria KG, Gunda S, Boddu SH, Mitra AK (2007) Novel approaches to retinal drug delivery. *Expert Opin Drug Deliv* 4:371–388.
36. Chang B, et al. (2002) Retinal degeneration mutants in the mouse. *Vision Res* 42: 517–525.
37. Yu DY, Cringle SJ (2006) Oxygen distribution in the mouse retina. *Invest Ophthalmol Vis Sci* 47:1109–1112.
38. Scarlatti F, et al. (2003) Resveratrol induces growth inhibition and apoptosis in metastatic breast cancer cells via de novo ceramide signaling. *FASEB J* 17:2339–2341.
39. Chattopadhyay A, London E (1988) Spectroscopic and ionization properties of *N*-(7-nitrobenz-2-oxa-1,3-diazol-4-yl)-labeled lipids in model membranes. *Biochim Biophys Acta* 938:24–34.
40. Gasco MR, Gasco P (2007) Nanovector. *Nanomedicine* 2:955–960.